



## CRACK FRONT WAVES

JOHN W. MORRISSEY and JAMES R. RICE\*

Division of Engineering and Applied Sciences and Department of Earth and Planetary Sciences,  
Harvard University, Cambridge, MA 02138, U.S.A.

(Received 15 July 1997)

### ABSTRACT

We present simulations of 3 D dynamic fracture which suggest that a persistent elastic wave is generated in response to a localized perturbation of a propagating crack front, e.g., by a local heterogeneity of critical fracture energy. The wave propagates along the moving crack front and spreads, relative to its origin point on the fractured surface, at a speed slightly below the Rayleigh speed. The simulations were done using the spectral elastodynamic methodology of Geubelle and Rice (1995). They model failure by a displacement-weakening cohesive model, which corresponds in the singular crack limit to crack growth at a critical fracture energy. Confirmation that crack front waves with properties like in our simulation do exist has been provided by Ramanathan and Fisher (1997). Through a derivation based on the linearized perturbation analysis of dynamic singular tensile crack growth by Willis and Movchan (1995), those authors found by numerical evaluation that a transfer function thereby introduced has a simple pole at a certain  $\omega/k$  ratio, corresponding to a non-dispersive wave. Further, we show that as a consequence of these persistent waves, when a crack grows through a region of small random fluctuations in fracture energy, the variances of both the local propagation velocity and the deformed slope of the crack front increase, according to linearized perturbation theory, in direct proportion to distance of growth into the randomly heterogeneous region. That rate of disordering is more rapid than the growth of the variances with the logarithm of distance established by Perrin and Rice (1994) for a model elastodynamic fracture theory based on a scalar wave equation. That scalar case, which shows slowly decaying (as  $t^{-1/2}$ ) rather than persistent crack front waves, is analyzed here too. © 1998 Elsevier Science Ltd. All rights reserved

Keywords: A. dynamic fracture, B. crack mechanics, B. stress waves, C. numerical algorithms.

### INTRODUCTION

When a crack propagates through a region of locally heterogeneous critical fracture energy, its front must speed up or slow down to accommodate those variations. This process creates elastic waves which interact with local stressing and fracture along other parts of the front. This paper addresses crack encounters with isolated regions of fracture energy heterogeneity, and shows that such interactions generate a previously unrecognized type of elastic wave which propagates along the moving crack front. Consequences are discussed for the growth of fluctuations in local speed and shape of the crack front during fracture propagation.

At the present level of modeling, the crack is confined to a plane and the medium through which it advances is assumed to be elastically homogeneous. Previous work (Perrin and Rice, 1994), based on a model scalar elastodynamic theory with linearized

\* To whom correspondence should be addressed.

perturbation of the crack front from a straight line (Rice *et al.*, 1994), showed that no statistically stationary crack configuration will exist under a sustained, small stationary random variation in critical fracture energy. The variances of both crack front slope and propagation velocity diverge logarithmically with distance of growth into the zone of variable toughness (although nonlinearities must ultimately saturate the fluctuations to a large-amplitude stationary distribution). The origin of the logarithmic divergence, discussed also by Ben-Zion and Morrissey (1995), is found in the asymptotic behavior of the space-time convolution kernel associated with wave-mediated stress transfer in the linearized perturbation analysis. That kernel decays as the inverse root of its argument for large arguments; its squared integral, arising in statistical analysis of the system, diverges logarithmically.

Of particular interest is the decay rate of signals produced in real vectorial elastodynamics by fracture energy fluctuations under Mode I (tensile) loading. We employ 3-D spectral computational methodology (Geubelle and Rice, 1995) to address such fluctuations in crack growth for Mode I cracks with a displacement-weakening failure criterion. The simulations of crack front interactions with inhomogeneities display long-lived signals produced by local fracture energy variations. These certainly decay more slowly than the inverse square root of travel distance, and seem not to totally decay, so as to represent persistent waves propagating along the moving crack front (Morrissey and Rice, 1996). The solution for the Mode I singular crack model with linearized perturbations in propagation speed has been developed by Willis and Movchan (1995). In support of the persistent crack front waves shown by our simulations, Ramanathan and Fisher (1997) have used the Willis–Movchan solution to extract a certain transfer function, that we call  $\hat{H}(k, \omega)$  subsequently ( $k$  = wave number along crack front,  $\omega$  = frequency), for crack growth at constant fracture energy. Their numerical evaluation of  $\hat{H}(k, \omega)$  confirms that it has a simple pole at a certain ratio  $\omega/k$ , corresponding to existence of a propagating mode at a wave speed comparable to what we found in the simulation.

It follows that the variances of small linearized fluctuations in crack front slope and velocity, in propagation through a region of small stationary random variation in fracture energy, diverge linearly with travel distance through the variable toughness zone for Mode I cracks in vectorial elasticity, rather than just logarithmically with travel distance as for the scalar theory.

## DYNAMIC CRACK MODELS

We consider an unbounded solid which contains a crack propagating on the plane  $y = 0$  (Fig. 1). Two formulations are discussed here:

- A model elastodynamic theory based on a scalar wave equation.
- Actual elastodynamic theory based on the vectorial Navier equations of motion.

The model theory involves a single displacement quantity  $u$  satisfying  $c^2 \nabla^2 u = u_{,tt}$  with associated stress  $\sigma = M u_{,y}$ , which vanishes on the fracture;  $M$  is an elastic modulus and  $c$  the wave speed. That formulation was used by Rice *et al.* (1994) and Perrin and Rice (1994) in the first studies of 3-D dynamic cracking through media of het-

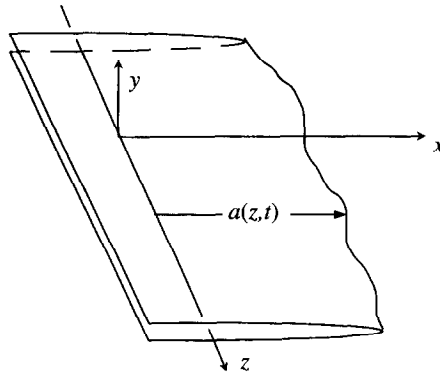


Fig. 1. Fracture on the plane  $y = 0$  in an unbounded solid.

erogeneous fracture toughness. The vectorial theory involves displacement vector  $\mathbf{u}$  satisfying  $(c_d^2 - c_s^2)\nabla(\nabla \cdot \mathbf{u}) + c_s^2 \nabla^2 \mathbf{u} = \mathbf{u}_{,tt}$ , with associated stresses  $\sigma_{\alpha\beta} = \bar{\lambda}(\nabla \cdot \mathbf{u})\delta_{\alpha\beta} + \mu(u_{\beta,\alpha} + u_{\alpha,\beta})$  of which  $\sigma_{yy} = \sigma_{yx} = \sigma_{yz} = 0$  on the fracture. Here  $\bar{\lambda}$  and  $\mu$  are the Lamé moduli,  $\mu$  being the shear modulus, and  $c_d$  and  $c_s$  are the dilatational and shear wave speeds, with  $c_d^2/c_s^2 = (\bar{\lambda} + 2\mu)/\mu$ .

For each of these formulations, the problem of spontaneous crack motion has been addressed, thus far, by two types of analysis :

- As a small perturbation from a straight crack front, and from propagation at uniform speed, for a half plane crack in an unbounded solid : In this case the singular crack model has been used and the solutions have been expressed in terms of perturbations to stress intensity factors  $K$  and energy release rate  $G$  along the crack front. Such solution was given for the scalar theory in Rice *et al.* (1994) and Perrin and Rice (1994), and was derived for vectorial elastodynamics by Willis and Movchan (1995) in the case of a mode I tensile crack, and by Movchan and Willis (1995) for modes II and III shear cracks. The analysis was recently extended to out-of-plane perturbations, not considered here, by Willis and Movchan (1997).
- As a non-perturbative numerical analysis of spontaneous fracture : In this approach a non-singular cohesive crack model of Barenblatt–Dugdale type has been adopted, as shown in Fig. 2, relating stress and relative displacement of the crack walls

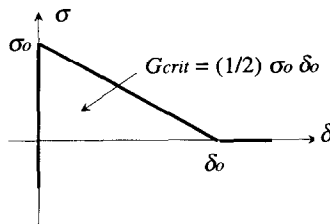


Fig. 2. Cohesive displacement–weakening relation between tensile stress  $\sigma$  and crack opening  $\delta$ . Fracture energy  $G_{crit}$  of corresponding singular crack model is equal to the area under the  $\sigma$  vs  $\delta$  relation ;  $G_{crit} = \sigma_0 \delta_0 / 2$  in this case.

through a displacement–weakening relation. This approach has been used by Guebbelle and Rice (1995), as an application of a spectral numerical methodology that they develop, and by Morrissey and Rice (1996) who noted the evidence of persistent crack front waves, for a mode I crack in vectorial elasticity, that we present here.

The non-singular displacement–weakening approach coincides with that based on the singular crack when the latter is formulated in terms of a critical fracture energy  $G_{\text{crit}}$ , where  $G_{\text{crit}}$  is the area identified in Fig. 2, at least in the case for which the size  $R$  of the zone over which displacement–weakening occurs is much smaller than other overall length scales in the fracture problem. In that range Rice [(1980); eqns (6.12) and (6.16)] shows that

$$R = R_{v=0}/f(v) \quad \text{where} \quad R_{v=0} \approx (9\pi/32)(M/\sigma_0)\delta_0. \quad (1)$$

Here  $M$  is the modulus of the model theory and is  $\mu/(1-\bar{\nu})$  for vectorial elasticity, where  $\bar{\nu} (= \bar{\lambda}/[2(\bar{\lambda} + \mu)])$  is the Poisson ratio. The function  $f(v)$ , where  $v$  is crack growth velocity, is unity when  $v = 0^+$  and increases to infinity at a limit speed  $v_{\text{limit}}$ , which is  $c$  for the scalar theory and is the Rayleigh speed  $c_R$  for vectorial elasticity. That is

$$f(v) = (1 - v^2/c^2)^{-1/2} (\text{scalar}), \quad \text{and} \quad f(v) = \frac{\alpha_d v^2}{(1 - \bar{\nu})r(v)c_s^2} (\text{vectorial mode I}), \quad (2)$$

where  $r(v) = 4\alpha_s\alpha_d - (1 + \alpha_2^2)^2$  is the Rayleigh function,  $\alpha_s = (1 - v^2/c_s^2)^{1/2}$ ,  $\alpha_d = (1 - v^2/c_d^2)^{1/2}$ , and  $c_s$  and  $c_d$  are the shear and dilatational wave speeds;  $r(c_R) = 0$ . We attempt here to choose parameters, within computer limitations, so that  $R$  is small compared to relevant scale lengths, but still large compared to the discretization size in the numerical formulation, so that our numerical solutions for cohesive crack models will be essentially indistinguishable from the corresponding singular crack solutions.

For the singular crack model, we know from the results of Kostrov (1966) and Eshelby (1969) for the scalar case, done as the mode III 2-D elastic problem, and of Freund (1972, 1990) for vectorial mode I, that the stress intensity factor  $K$  has the mathematical structure

$$K = \hat{k}(v)K_{\text{rest}} \quad (3)$$

where  $\hat{k}(v)$  is a universal function of instantaneous crack speed  $v$ , with  $\hat{k}(0) = 1$  and  $\hat{k}(v_{\text{limit}}) = 0$ , and where the “rest” value of  $K$ , to which it would revert if the crack growth were suddenly stopped, is  $K_{\text{rest}}$ ;  $K_{\text{rest}}$  is a functional of the history of crack motion up to the present. It has a very simple form, emphasized by Eshelby (1969) and Freund (1972), when the crack front is straight (2-D problem) and when only outgoing waves are involved, without effect of reflections from boundaries or from the opposite end of the crack. Here  $\hat{k}(v)$  is

$$\hat{k}(v) = (1 - v/c^{1/2}) (\text{scalar}), \quad \text{and} \quad \hat{k}(v) = \frac{1 - v/c_R}{S_+ (1/v)(1 - v/c_d)^{1/2}} (\text{vectorial mode I}), \quad (4)$$

Table 1. Values of the Freund (1972, 1990) slowness function  $S_+(1/v)$  for various crack speeds  $v$ , for a range of values of Poisson ratio  $\bar{\nu}$

$\bar{\nu}$	0.15000	0.20000	0.25000	0.30000	0.35000	0.40000
$c_R/c_s$	0.90222	0.91100	0.91940	0.92741	0.93501	0.94220
$v/c_R = 0$	1.0000	1.0000	1.0000	1.0000	1.0000	1.0000
$v/c_R = 0.1$	0.98600	0.98459	0.98308	0.98147	0.97979	0.97806
$v/c_R = 0.2$	0.96989	0.96689	0.96370	0.96032	0.95681	0.95321
$v/c_R = 0.3$	0.95113	0.94635	0.94127	0.93594	0.93041	0.92480
$v/c_R = 0.4$	0.92899	0.92217	0.91498	0.90746	0.89973	0.89193
$v/c_R = 0.5$	0.90243	0.89328	0.88367	0.87371	0.86354	0.85336
$v/c_R = 0.6$	0.86992	0.85804	0.84566	0.83293	0.82005	0.80726
$v/c_R = 0.7$	0.82906	0.81393	0.79831	0.78241	0.76646	0.75079
$v/c_R = 0.8$	0.77580	0.75669	0.73718	0.71753	0.69804	0.67908
$v/c_R = 0.9$	0.70248	0.67819	0.65368	0.62928	0.60538	0.58236
$v/c_R = 1.0$	0.59093	0.55851	0.52606	0.49399	0.46267	0.43243

where the slowness function  $S_+(1/v)$  is an integral arising from the Wiener–Hopf factorization for the moving crack problem by Freund (1972: p. 133, eqn (2.19); 1990: p. 347, eqn (6.4.18)). Freund (1990: p. 349) notes that  $S_+(\infty) = 1$  and that  $S_+(1/v)$  is “not too different from unity over the full range of its argument”. The most compact means of evaluation seems to follow from a transformation by Freund (1990: p. 347, eqn (6.4.20); p. 88, eqn (2.5.29); p. 349) to another function  $S_-^0(1/v)$ , which arises in Wiener–Hopf factorization for a non-growing crack, and this shows that

$$\begin{aligned}
 S_+(1/v) &= 1/S_-^0(1/v) = \exp \left[ \frac{1}{\pi} \int_{1/c_d}^{1/c_s} \tan^{-1} \left\{ \frac{4\eta^2 \sqrt{[\eta^2 - (1/c_d)^2][(1/c_s)^2 - \eta^2]}}{[2\eta^2 - (1/c_s)^2]^2} \right\} \frac{d\eta}{\eta - 1/v} \right] \\
 &= \exp \left[ -\frac{v}{\pi} \int_{c_s}^{c_d} \tan^{-1} \left\{ \frac{4\sqrt{(1 - c^2/c_d^2)(c^2/c_s^2 - 1)}}{(2 - c^2/c_s^2)^2} \right\} \frac{dc}{c(c-v)} \right]. \quad (5)
 \end{aligned}$$

We show results for  $S_+(1/v)$  as a function of  $v$ , for several values of  $\bar{\nu}$ , in Table 1.

The energy release rate has the mathematical form

$$G = f(v)K^2/2M, \quad (6)$$

where  $f(v)$  and  $M$  are the same as earlier, and thus one has

$$G = g(v)G_{\text{rest}} \quad (7)$$

where  $G_{\text{rest}} \equiv K_{\text{rest}}^2/2M$  is the rest value of the energy release rate, a functional of prior growth history, and where  $g(v) = f(v)/[k(v)]^2$ . This function  $g(v)$  satisfies  $g(0^+) = 1$  and  $g(v_{\text{limit}}) = 0$ ; specific forms are

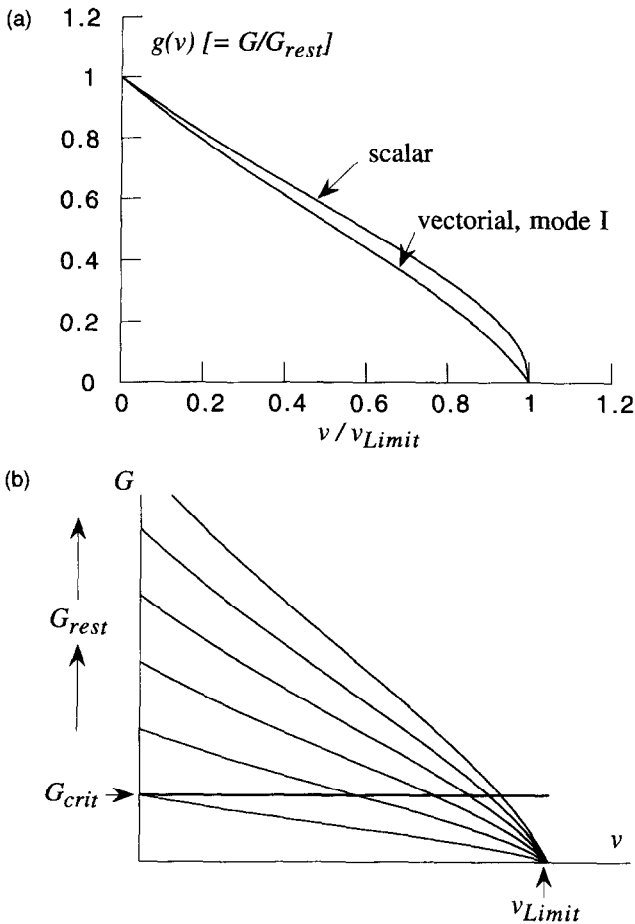


Fig. 3. (a) Illustration of relation  $G = g(v)G_{rest}$  between energy release rate  $G$  (per unit crack area), crack speed  $v$ , and rest value  $G_{rest}$  of  $G$ ;  $v_{limit} = c$  for scalar model,  $v_{limit} = c_R$  for vectorial mode I; for vectorial case,  $\bar{\nu} = 0.25$ . (b) Also shown: How crack growth at constant  $G (=G_{crit})$  but steadily increasing  $G_{rest}$  causes  $v$  to accelerate towards  $v_{limit}$ .

$$g(v) = [(1 - v/c)/(1 + v/c)]^{1/2} (\text{scalar}), \quad \text{and} \quad g(v) \approx 1 - v/c_R (\text{vectorial mode I})$$

(8)

where the latter is an approximation suggested by Freund based on his plots of  $g(v)$  (Freund, 1972: p. 139, Fig. 4; Freund, 1990: p. 349, Fig. 6.10). Figure 3a shows both  $g(v)$  functions, with the exact one plotted in the vectorial case, for  $\bar{\nu} = 0.25$ . Figure 3b indicates that if, like in typical situations for enlarging cracks under remote loading,  $G_{rest}$  increases as the crack grows, and if that growth is, e.g., at a constant  $G = G_{crit}$ , then  $v$  accelerates towards  $v_{limit}$ . Of course, real cracks will bifurcate away from the assumed planar path well before  $v$  approaches  $v_{limit}$ , unless channeled by a weakly bonded interface (Washabaugh and Knaus, 1994).

## SIMULATION METHODOLOGY

In order to implement the non-singular cohesive model, with displacement–weakening, we follow the spectral numerical methodology of Geubelle and Rice (1995). Assuming that the fracture takes place on the plane  $y = 0$  separating identical elastic half spaces, they show that the following equation in vectorial elastodynamics, for mode I, relates tensile stress  $\sigma(x, z, t)$  ( $\equiv \sigma_{yy}(x, 0, z, t)$ ), acting perpendicular to the interface  $y = 0$ , to the opening displacement discontinuity  $\delta(x, z, t)$  there:

$$\sigma(x, z, t) = \sigma^0(x, z, t) - \frac{\bar{\lambda} + 2\mu}{2c_d} \frac{\partial \delta(x, z, t)}{\partial t} + \phi(x, z, t). \quad (9)$$

Here  $\delta(x, z, t) = u(x, 0^+, z, t) - u(x, 0^-, z, t)$ , where  $u(\equiv u_i)$  is displacement in a direction perpendicular to the interface,  $\sigma^0(x, z, t)$  is the stress which external loading would transmit to that interface if it was constrained against any opening (i.e., if  $\delta$  was constrained to be uniformly zero), and  $\phi(x, z, t)$  is a functional which depends on the prior history of opening  $\delta(x', z', t')$  for all  $x', z', t'$  within the wave cone of  $x, z, t$ . The numerical method that we employ adopts a spectral representation of both  $\delta$  and  $\phi$ , as a Fourier sum over wave numbers  $k$  and  $m$ ,

$$\begin{cases} \delta(x, z, t) \\ \phi(x, z, t) \end{cases} = \sum_{k,m} \begin{cases} D(k, m, t) \\ F(k, m, t) \end{cases} e^{i(kx + mz)}, \quad (10)$$

where the Fourier coefficients are related by (Geubelle and Rice, 1995)

$$F(k, m, t) = -\frac{1}{2} q^2 c_s \int_0^t h(qc_s(t-t')) D(k, m, t') dt' \quad (11)$$

with  $q = \sqrt{k^2 + m^2}$  and

$$h(T) = \mu C_1(T) = \mu \left[ \beta^2 \frac{J_1(\beta T)}{T} - 4T \int_T^{\beta T} \frac{J_1(T')}{T'} dT' + \beta(4 - \beta^2) J_0(\beta T) - 4J_0(T) \right]. \quad (12)$$

Here  $J_0$  and  $J_1$  are Bessel functions of the first kind, and  $\beta^2 = c_d^2/c_s^2 = (\bar{\lambda} + 2\mu)/\mu$ .

For the scalar theory, the same formulation applies but now  $(\bar{\lambda} + 2\mu)/2c_d$  in eqn (9) is replaced by  $M/2c$ ,  $c_s$  in eqn (11) is replaced by  $c$ , and the convolution kernel there is replaced by  $h(T) = MJ_1(T)/T$ . The relation between  $\phi(x, z, t)$  and  $\delta(x, z, t)$ , in both scalar and vector cases, can also be expressed as space-time convolution integrals given by Cochard and Rice (1997).

In the numerical implementation we select a region of the  $x$ - $z$  plane, Fig. 4, of extent  $\lambda_z = \lambda$  in the  $z$  direction and  $\lambda_x = 2\lambda$  in the  $x$ -direction, and cover it with a grid of  $N_z$  ( $= 512$  for scalar,  $1024$  for vectorial) points in the  $z$  direction, and  $N_x$  ( $= 1024$  for scalar,  $2048$  for vectorial) points in the  $x$  direction. Regarding these as Fast Fourier Transform (FFT) sample points, this corresponds to selecting wave numbers  $k = 2\pi j/\lambda_x$  and  $m = 2\pi l/\lambda_z$ , with  $j$  ranging over all integers from  $-N_x/2$  to  $N_x/2$  and  $l$  from  $-N_z/2$  to  $N_z/2$ , in truncated Fourier series representations of  $\delta$  and  $\phi$  like in eqn

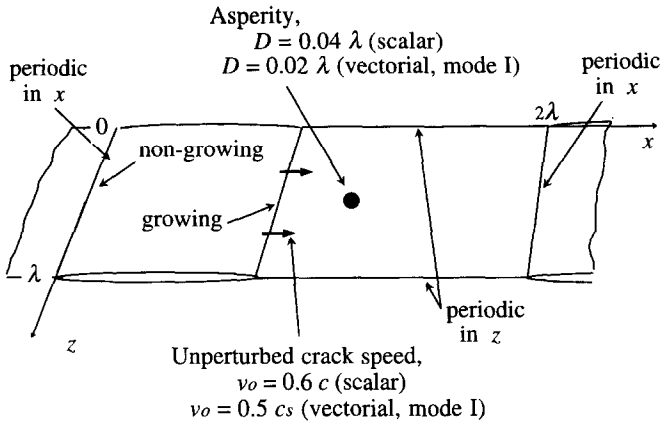


Fig. 4. Simulation domain, replicated with periodic length  $\lambda$  in the  $z$  direction, along the crack front, and  $2\lambda$  in the  $x$  direction. Critical fracture energy  $G_{\text{crit}}$  (and  $\sigma_0$  and  $\delta_0$ ) are constant everywhere ahead of the pre-crack, except for the asperity region where  $\sigma_0$  and  $\delta_0$  are increased by 5%, hence  $G_{\text{crit}}$  by 10%. The loading  $\sigma^0(x, t)$  is chosen to give an approximately constant crack growth rate  $v_0$  in absence of the asperity. A narrow strip of high  $\sigma_0$  at the crack border near  $x = 0$ , and its periodic replicates, prevents propagation in the negative  $x$  direction.

(10). Hence, whatever rupture process happens over this domain, of extent  $\lambda_x$  by  $\lambda_z$ , is replicated periodically in the two spatial directions, with respective periods  $\lambda_x$  and  $\lambda_z$ . Thus we are interested in results of the calculation up until the arrival of waves from the replicate regions. Cochar and Rice (1997) show how to eliminate these replication effects rigorously in a formulation that retains the spectral basis and modal independence of the convolution, but at the expense of far more elaborate calculations, not yet implemented in code for vectorial elasticity, to obtain the convolution kernels.

As illustrated in Fig. 4, the problem we address is one for which an initial crack exists of 2-D form so that, if the loading is independent of  $z$ , as we assume, and if the fracture properties are uniform, the fracture would grow with a straight front under 2-D plane strain conditions in the  $x$ - $y$  plane. However, our focus here is on the effect of small heterogeneities in fracture toughness, so that the crack front is slightly perturbed from straight. This is to provide solutions to compare with the analytical works on linearized perturbation mentioned, and particularly to learn how the Perrin and Rice (1994) analysis of disorder in growth may extend to the vectorial case. [Geubelle and Rice (1995) show an application of the methodology to far stronger perturbations of toughness, nearly sufficient to arrest a running crack.] The fracture properties  $\sigma_0$  and  $\delta_0$  are taken as uniform everywhere except within the small asperity region identified, where both are increased by 5%, so that the fracture energy is increased from  $G_{\text{crit}}$  to  $1.1 G_{\text{crit}}$  within the asperity. To disallow fracture propagation for the end of the crack near  $x = 0$ , and its periodic replicates,  $\sigma_0$  is assigned large values in a narrow strip which borders it. The asperity diameter  $D$  is chosen as  $20h$  in all cases, where  $h$  is the FFT sample point spacing, that is,  $h = \lambda/N_z = 2\lambda/N_x$ . Thus  $D = 0.04\lambda$  in the scalar and  $0.02\lambda$  in the vectorial simulation. Further, we choose the parameter combination  $M\delta_0/\sigma_0$  in the scalar case, and  $\mu\delta_0/(1-\bar{\nu})\sigma_0$  in the vectorial, so that the nominal cohesive zone size is  $R_{v=0} = 8h$  in both cases.

The loading  $\sigma^0(x, z, t)$  is chosen so that, for a calibration run in absence of any asperity region, the crack speed would be nearly constant at  $v_0$ , chosen as  $v_0 = 0.6c$  in the scalar case to be shown here, and  $v_0 = 0.5c_s$  in the vectorial. Loadings of the type  $\sigma^0 \propto 1/\sqrt{t}$  can accomplish growth at constant speed, within the singular crack model, for cracks which begin at zero length. The cracks in the simulations begin at finite length  $a_{\text{init}} = 64h$  ( $=\lambda/8$  in the scalar case and  $\lambda/16$  in the vectorial) and are non-singular cracks. We stipulate that  $\sigma = 0$  on the initial crack  $0 < x < a_{\text{init}}$  for all time  $t > 0$ , and we let the cohesive law apply outside the crack. We let  $a(t)$  mark the furthest extent of the decohering zone (i.e., the zone where  $\sigma$  has previously reached the strength  $\sigma_0$  and is now undergoing displacement weakening) in the calibration run;  $a(0^+) = a_{\text{init}}$ , and we apply the loading stress  $\sigma^0(x, t)$  for  $t > 0$  as

$$\sigma^0(x, z, t) = \begin{cases} \text{constant} \times \sqrt{\frac{2M\sigma_0\delta_0}{\pi a(t)}} & \text{for } 0 < x < a(t) \\ 0 & \text{for } a(t) < x < 2\lambda \end{cases} \quad (13)$$

Here  $M$  is the modulus of the scalar theory and is replaced by  $\mu/(1-\bar{\nu})$  in the vectorial mode I case. Choice of the constant equal to unity in this equation corresponds to the static crack growth threshold for the corresponding singular crack model with fracture energy  $G_{\text{crit}} = \sigma_0\delta_0/2$ , for an isolated tunnel crack of length  $a(t)$ . Choice of greater values of the constant corresponds to dynamic crack motion. We found in such cases that after an initial transient the crack speed  $v(t) \equiv da(t)/dt$  settled down to a nearly constant value (within about  $\pm 5\%$ ) despite wave reflections from the crack end blocked at  $x = 0$ , at least until relatively large times when stress pulses arrived from the periodic replicates of the fracture process. We chose the constant by trial and error to give the unperturbed speeds noted above.

In application to the fully 3-D simulations with the asperity zone present, the same constant was used and the loading history was as described above, but with the non-zero value of  $\sigma^0(x, z, t)$  now applying for  $0 < x < a(z, t)$ , where  $a(z, t)$  is the local crack depth (Fig. 1). Again, we specify  $\sigma = 0$  for all time on the initial crack, whereas the rest of the medium follows the stress–displacement law once the stress  $\sigma_0$  (or  $1.05\sigma_0$  in the asperity) has been attained. The constitutive relation is imposed only at the FFT sample points, which are equal in number to the number of Fourier modes in the spectral sum.

The time step  $\Delta t$  chosen in  $0.5h/c$  in the scalar case, and  $0.5h/c_s$  in the vectorial. To understand the computational procedure, consider a moment  $t$  in the history at which the opening displacement  $\delta(x, z, t)$  has been determined by calculations up to that time. We need to determine  $\phi(x, z, t)$  also, and we obtain that by doing the following three operations:

- (i) Do an FFT to go from  $\delta(x, z, t)$  at its sample points  $x, z$  to the modal components  $D(k, m, t)$  for all wave numbers  $k, m$  in the truncated Fourier sum.
- (ii) Making use also of all prior  $D(k, m, t')$ ,  $t' < t$ , perform the convolutions for each Fourier mode to get  $F(k, m, t)$ .
- (iii) Do an inverse FFT to go from the  $F(k, m, t)$  to  $\phi(x, z, t)$  at the sample points.

From the then known  $\phi(x, z, t)$ , and from evaluating  $\sigma(x, z, t)$  in terms of  $\delta(x, z, t)$  according to the displacement weakening constitutive law, use can be made of eqn (9) to calculate the opening velocity  $\partial\delta(x, z, t)/\partial t$  at all sample points. We then step  $\delta(x, z, t)$  to a new value  $\delta(x, z, t + \Delta t) = \delta(x, z, t) + \Delta t \partial\delta(x, z, t)/\partial t$ , at  $t + \Delta t$  at the sample points, and then the process just described begins anew.

Most of the computer time is spent on the convolutions, step (ii) above. They can be done completely in parallel without processor communication. So the methodology is well suited to highly parallel computer architectures, with large amounts of memory. We used the CM-5 Connection Machine. The convolution integrals have the structure  $F(t) = -\int_0^t H(t-t')D(t') dt'$  (omitting explicit reference to wave numbers and absorbing constants into a new function definition  $H(t) \equiv (1/2)q^2 c_s h(qc_s t)$  for the kernel). We wish to evaluate  $F_n \equiv F(n\Delta t)$  in terms of the known sequence  $D_m \equiv D(m\Delta t)$ ,  $m = 1, 2, \dots, n$ , where  $D_m \equiv 0$ ,  $m \leq 0$ . We followed the procedure of Morrissey and Geubelle (1997), first storing arrays of pre-integrated kernel values

$$K_n = (\Delta t/2)[H((n+d)\Delta t) + H((n-1+d)\Delta t)] \quad \text{for } n = 1 \text{ to } n_{\max}, \quad (14)$$

where  $n_{\max}$  is the largest number of steps in the calculation, and then evaluating

$$F_n = -\sum_{m=1}^n K_{n+1-m} D_m. \quad (15)$$

Here  $d$  is a delay factor which, based on the Morrissey and Geubelle (1997) suggestions from studies of numerical precision and stability of the procedure, we take as  $d = 1/2$  in the scalar case and  $d = 0$  in the vectorial case. Further details of the methodology follow Geubelle and Rice (1995), who used the same displacement–weakening model.

## RESULTS

The asperity encounter induces a local fluctuation in speed of the fracture front, which propagates along the front as it moves. We determine the local fracture velocity at the fracture front, to obtain the difference  $V(z, t) \equiv v(z, t) - v_0$  between the local and unperturbed velocity (where we take  $v_0$  as the very slightly time-dependent speed in the calibration run with straight crack front discussed above). It is perhaps more fundamental to think of results as a perturbation in  $G_{\text{rest}}$  which would, in absence of the asperity, be uniform along the then straight crack front, and be nearly (within simulation accuracy) uniform in time. The crack grows in a region of uniform  $G_{\text{crit}}$  after passing the asperity, so that  $G_{\text{crit}} = g(v)G_{\text{rest}}$  is constant, and hence the fluctuations are related by

$$\Delta G_{\text{rest}}(z, t) = -[g'(v_0)/g^2(v_0)]G_{\text{crit}}V(z, t). \quad (16)$$

Note that the bracketed term is negative so that both fluctuations are of the same sign.

We show plots of  $\Delta G_{\text{rest}}/\Delta G_{\text{crit}}$  (where  $\Delta G_{\text{crit}} = 0.1G_{\text{crit}}$  in this case) vs distance  $z$  along the crack front at a series of equally spaced times  $t$  after the asperity encounter, so that the quantity plotted is  $\Delta G_{\text{rest}}/\Delta G_{\text{crit}} + \text{constant} \times t$ . This conveys the notion that

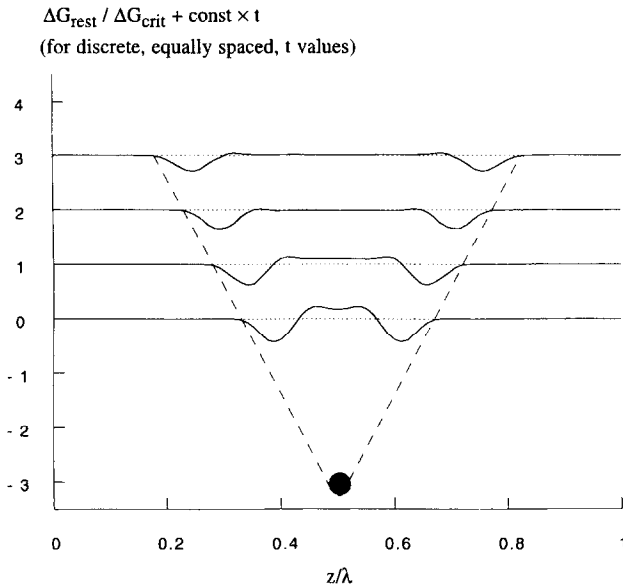


Fig. 5. Results for model elastodynamic theory based on scalar wave equation. Perturbation of conditions along the crack front, due to asperity encounter, shown by plotting  $\Delta G_{\text{rest}}(z, t) + \text{constant} \times t$  vs  $z$ ;  $\Delta G_{\text{rest}}$  is proportional to the local perturbation  $V(z, t)$  of crack speed. For this scalar case the wave of disturbance, propagating along the moving crack, slowly decays, as  $t^{-1/2}$ . Dashed lines represent locus of intersections of spherical wave front, growing from asperity location at speed  $c$ , with the moving crack front.

the crack front, where not yet influenced by waves from the asperity encounter, is advancing uniformly with time.

*Crack in a scalar elastic solid:* Figure 5 depicts pulses that are created by the crack encounter with the asperity. The dashed lines in the figure show where body waves of speed  $c$ , originating from the asperity, would intersect the future crack front. The pulse size decreases with propagation and the pulse travels with the wave speed  $c$  relative to the asperity site. That corresponds to speed  $\sqrt{c^2 - v_0^2}$  as measured in the direction parallel to the crack front. Since we had a tougher asperity rather than a more brittle zone, most of the signal is to slow  $v$  down rather than speed it up. So, in terms of the resulting perturbation of crack front position, this results in a gentle propagating kink.

Figure 6a shows the amplitude (measured from peak to trough) of the disturbance of Fig. 5 vs normalized time  $ct/D$  ( $D =$  asperity diameter). The disturbance is seen to decay. The decay is initially rapid but slows down after the pulse has traveled 10 asperity diameters. There is some noise in the measure of the amplitude because the measure chosen is very simple. A more sophisticated measure would probably smooth this out. Figure 6b is a logarithmic plot of the same results. This lets us obtain an exponent of the decay rate of the amplitude of the pulse, which is seen to be well described by decay in proportion to  $t^{-1/2}$ . This is the result expected from the linearized perturbation analysis for the scalar case (Rice *et al.*, 1994; Perrin and Rice, 1994), which is that long after the asperity encounter the perturbation  $v(z, t) - v_0$  should

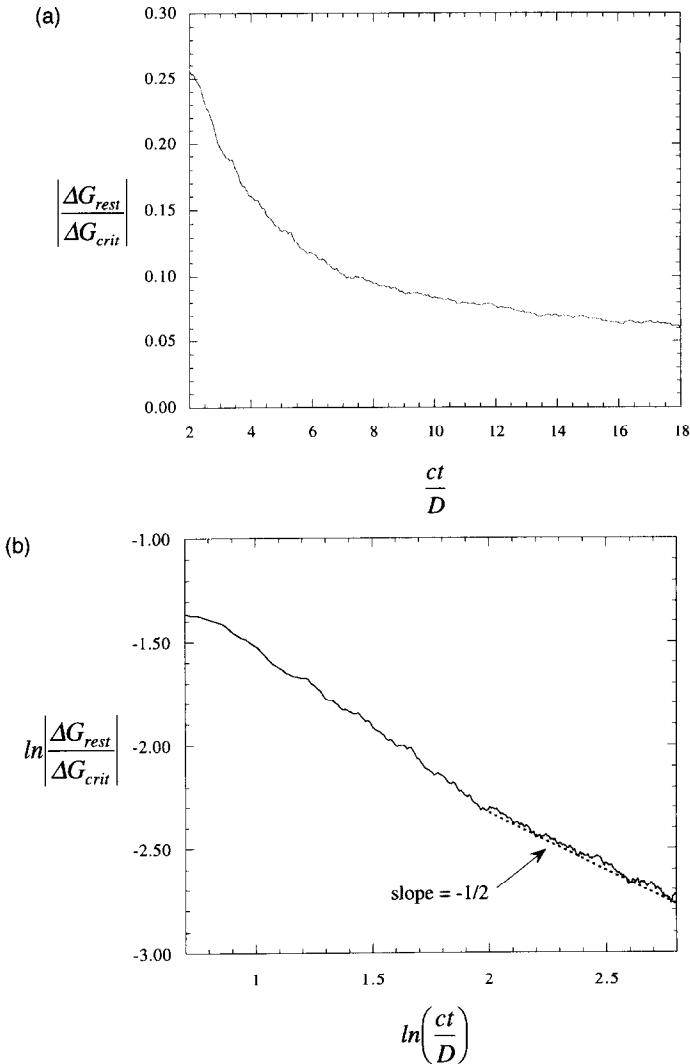


Fig. 6. Decay of the amplitude (measured from peak to trough) of  $\Delta G_{rest}$  shown (a) on linear scale, and (b) on logarithmic scale, for the scalar case. Here  $D$  is the asperity diameter. The plot in (b) confirms the theoretical prediction of pulse amplitude decay as  $t^{-1/2}$ .

decay as  $t^{-1/2}$  in a pulse which spreads laterally along the crack front at speed  $\sqrt{c^2 - v_0^2}$ . Such may be deduced from the result (Perrin and Rice, 1994) for perturbation in crack front position as

$$a(z, t) - v_0 t = - \frac{\alpha_0^2 c}{\pi G_{crit,0}} \int_0^t \int_{z - \alpha_0 c(t-t')}^{z + \alpha_0 c(t-t')} \frac{\Delta G_{crit}(v_0 t', z')}{\sqrt{\alpha_0^2 c^2 (t-t')^2 - (z-z')^2}} dz' dt' \quad (17)$$

for growth into a region, beginning at  $x = 0$ , in which the critical fracture energy is

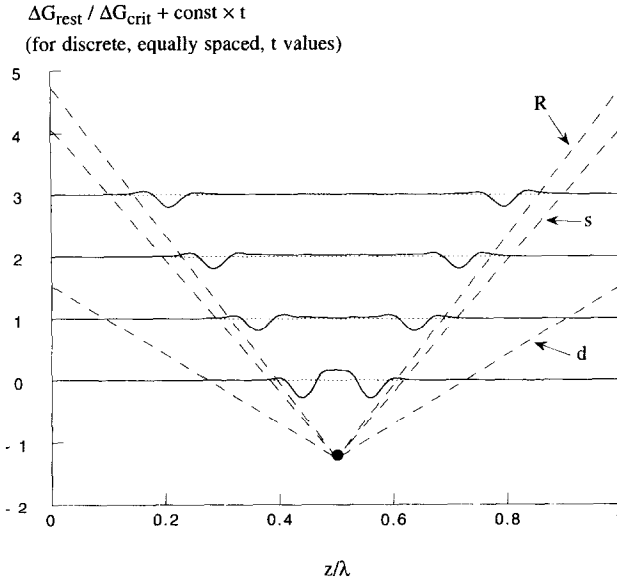


Fig. 7. Results for mode I crack in vectorial elastodynamics, showing persistent crack front waves generated by the asperity encounter. Perturbation of conditions along the crack front shown by plotting  $\Delta G_{\text{rest}}(z, t) + \text{constant} \times t$  vs  $z$ ;  $\Delta G_{\text{rest}}$  is proportional to the local perturbation  $V$  of crack speed. Dashed lines represent the intersections of spherical wave fronts of dilatational and shear waves, and of circular front of Rayleigh surface wave, with the moving crack front. The persistent wave appears to move (relative to the source asperity) slightly slower than the Rayleigh speed.

perturbed by  $\Delta G_{\text{crit}}(x, z)$  from its uniform value  $G_{\text{crit},0}$ , prevailing for  $x < 0$  and leading there to unperturbed crack speed  $v_0$ . Here,  $\alpha_0 = (1 - v_0^2/c^2)^{1/2}$  and the half plane crack grows under loading conditions such that  $G_{\text{rest}}$  has a constant value, equal to  $[(1 + v_0/c)/(1 - v_0/c)]^{1/2} G_{\text{crit},0}$ , so long as the crack front remains straight.

*Crack in a vectorial elastic solid, mode I:* Figure 7 shows the simulation result for  $\Delta G_{\text{rest}}/\Delta G_{\text{crit}}$  (or, essentially,  $V$ ), for the vectorial elasticity mode I case. Now we see that the pulses spreading along the crack front are long-lived with no evident tendency for decay, or at least for decay with rapidity comparable to the scalar case. Lines in the figure show where shear and dilatational body waves, and Rayleigh surface waves, originating from the asperity would intersect the crack front. The dilatational wave arrival has no discernible effect on the crack and the disturbance seems to begin with the shear arrival. The long-lived pulse seems to propagate at a speed, relative to the asperity, which is very close to, but slightly less than, the Rayleigh speed.

Figure 8a shows the amplitude of the disturbance (measured peak to trough) vs normalized time. This confirms that, in contrast to the scalar elastic case shown in Fig. 6, the disturbance does not seem to decay, but rather represents a persistent wave which spreads along the growing crack front. When we take the logarithm of the mode I results, as is done in Fig. 8b, it appears that there is initially a decay proportional to  $t^{-1/2}$  just like in Fig. 6b.

The existence of crack front waves in the vectorial case may be directly verified

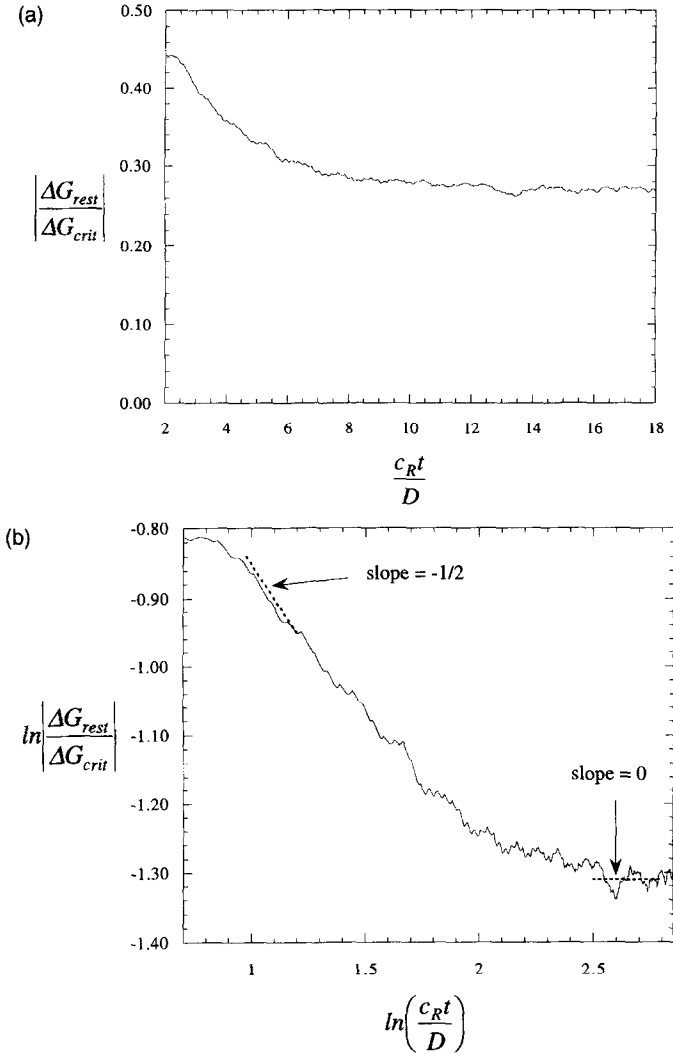


Fig. 8. Decay of amplitude (measured peak to trough) of  $\Delta G_{rest}$  shown (a) on a linear scale, and (b) on a logarithmic scale, for the vectorial mode I case. Here  $D$  is the asperity diameter. The plot in (a) shows the persistence of the crack front waves. That in (b) suggests that the early history of the response may decay approximately as  $t^{-1/2}$  like for the scalar case.

based on the Willis and Movchan (1995) linear perturbation solution for the singular crack model. This involves a half plane crack in an unbounded solid, growing under conditions for which  $K_{rest}$  and  $G_{rest}$  are constant when the crack front remains straight, the same case considered by Rice *et al.* (1994) for the scalar model. Let the crack front position perturbation  $A(z, t) \equiv a(z, t) - v_0 t$  have space-time Fourier transform

$$\hat{A}(k, \omega) = \int_{-\infty}^{+\infty} \int_{-\infty}^{+\infty} e^{-ikz - i\omega t} A(z, t) dz dt \quad (18)$$

and use similar notation for the transform  $\Delta\hat{K}(k, \omega)$  of the corresponding stress intensity factor perturbation from its unperturbed value  $K_0$ . Willis and Movchan (1995) show that

$$\Delta\hat{K}(k, \omega)/K_0 = |k|F(\omega/|k|, v_0)\hat{A}(k, \omega), \quad (19)$$

where  $F(\omega/|k|, v_0)$  is given by an expression involving an integral [their eqns (8.10) and (9.7)–(9.12)] that does not allow simple evaluation. Since  $G = f(v)K^2/2M$ , the corresponding perturbation in  $G$  is

$$\Delta G(z, t)/G_0 = [f'(v_0)/f(v_0)]V(z, t) + 2\Delta K(z, t)/K_0, \quad (20)$$

where  $V(z, t) = \partial A(z, t)/\partial t$ . Thus writing  $\hat{V}(k, \omega) = i\omega\hat{A}(k, \omega)$ , the Willis–Movchan solution implies that the perturbation of  $G$  is

$$\Delta\hat{G}(k, \omega)/G_0 = 2\hat{A}(k, \omega)/\hat{H}(k, \omega), \quad (21)$$

where the transfer function  $\hat{H}(k, \omega)$ , relating a perturbation of  $G$  (which we regard as given through a specified, slightly non-uniform,  $G_{\text{crit}}$  distribution) to the resulting perturbation  $A$  of crack motion is

$$\hat{H}(k, \omega) = \frac{2/|k|}{[f'(v_0)/f(v_0)]i\omega/|k| + 2F(\omega/|k|, v_0)}. \quad (22)$$

Ramanathan and Fisher (1997) have numerically evaluated an expression which should be equivalent and thus shown that  $\hat{H}(k, \omega)$  has a simple pole at a certain real value of  $\omega/k$ . That confirms the existence of a propagating mode for crack growth at constant fracture energy. The critical  $\omega/k$  corresponds to the speed  $\sqrt{c_f^2 - v_0^2}$  at which such waves propagate in the direction parallel to the crack front, which is moving itself at the (unperturbed) speed  $v_0$ . With such notation,  $c_f$  is the speed relative to a fixed point on the fractured surface from which the wave originated, and  $\sqrt{c_R^2 - v_0^2}$  is the corresponding lateral speed of a Rayleigh wave from the same source. For  $\bar{\lambda} = \mu$  ( $\bar{\nu} = 1/4$ ), Ramanathan and Fisher (1997) report that  $\sqrt{c_f^2 - v_0^2}/\sqrt{c_R^2 - v_0^2}$  varies from about 0.94–1.00 as the unperturbed crack speed  $v_0$  varies from 0 to  $c_R$ . These results are consistent with our simulation, Fig. 7. Ramanathan and Fisher further note that the crack front wave exists only when the propagation criterion is one of constant  $G_{\text{crit}}$ , which is the singular-crack case to which our non-singular displacement weakening model corresponds. That is the case in which the fracture model forms a dynamically conservative system. Further, if  $G_{\text{crit}}$  is instead assumed to depend on velocity  $v$  of crack propagation, Ramanathan and Fisher show that the pole moves off the real  $\omega/k$  axis such that assumption of  $dG_{\text{crit}}/dv > 0$  attenuates the crack front wave, whereas  $dG_{\text{crit}}/dv < 0$  results in unstable amplification.

## DISCUSSION : CRACK FRONT WAVES AND STATISTICS OF DISORDERING

Perrin and Rice (1994) showed how to calculate, in the scalar case, the space-wise power spectrum and correlation function for position of a singular crack front which grows through a region, beginning at  $x = 0$  and  $t = 0$ , of small but statistically

stationary random fluctuation in fracture energy. They showed that, within the linear perturbation analysis, the crack front never attains a statistically stationary configuration. Rather, the variances of such quantities as the local velocity fluctuation  $V(z, t) = v(z, t) - v_0$ , or local slope  $S(z, t) = \partial a(z, t) / \partial z$  of the crack front, increase without limit. This increase is very gradual in time, as  $\log(t)$ .

The non-existence of a statistically stationary limit, within the linear perturbation analysis, was pointed out by Rice *et al.* (1994) and Perrin and Rice (1994) to be due to the slow (as  $t^{-1/2}$ ) decay of the response to perturbation, as illustrated in Figs 5 and 6. We have now seen that the response to perturbation in the vectorial elastic case does, in fact, not decay at all. So there too, no statistically stationary state of the perturbed crack front will be achieved and there will be a more vigorous growth of the variances of  $V$  and  $S$ . Indeed, these must grow in direct proportion to distance of propagation into the heterogeneous region, as now discussed.

We present a simplified analysis of the statistics of such disordering here; the outline of a rigorous discussion in the style of Perrin and Rice (1994) is given in the next section. Assume that  $G_{\text{crit}}$  is uniform on the domain  $x < 0$  of the fracture plane but contains small random fluctuation from that uniform value on  $x > 0$ . The random distribution has correlation length scale  $b$ , so we can think of the heterogeneities, approximately, as small asperities, each of area  $b^2$ , which are uncorrelated with one another. The crack propagates at uniform speed  $v_0$  over the domain  $x < 0$  and then, upon reaching  $x = 0$ , begins to be perturbed. The net result is an excitation of the crack front by each of the asperities that have been encountered, whose effect we can sum linearly. Each asperity creates a pair of pulses which decay in the scalar theory (Fig. 5) but are persistent in the vectorial case (Fig. 7). We may say that the velocity perturbation in the pulse generated by a single asperity, representing a unit perturbation in  $G_{\text{crit}}$ , decays long afterwards as  $\eta(b/v_0 t')^p$  where  $\eta$  is a factor,  $t'$  is time since the asperity encounter, and where  $p = 1/2$  for the scalar model but  $p = 0$  for vectorial elastodynamics (persistent pulse).

The net velocity fluctuation  $V$  at some position  $z$  along the crack front is the sum of effects from all previously encountered asperities whose pulses happen to be passing by  $z$  at the moment considered. After a time  $t$  of propagation, the crack will have traversed  $n = v_0 t / b$  rows of such asperities. An asperity having a  $G_{\text{crit}}$  perturbation of  $R_k$ , encountered  $k$  rows before the present crack front position, at time  $t' = kb/v_0$  before  $t$  will therefore generate a pulse of amplitude  $\eta k^{-p} R_k$ , at least at reasonably large  $k$ , along the crack front at time  $t$ . Thus, summing the effects of those asperities from each row which can deliver a pulse to  $z$  at time  $t$ , we generate the fluctuation

$$V \approx \sum_{k=1}^n \eta k^{-p} (R_k + R'_k) \quad (23)$$

there. This recognizes that for each  $k$ , there are two asperities, one of strength  $R_k$  at a position  $z' < z$  and one of strength  $R'_k$  at a  $z' > z$ , which can deliver pulses to  $z$ . Thus, since all the  $R_k$  and  $R'_k$  are identically distributed and statistically independent,  $E(R_k R_l) = E(R'_k R'_l) = \delta_{kl} \hat{R}^2$ , and  $E(R_k R'_l) = 0$ , where  $\hat{R}$  is the r.m.s. fluctuation in  $G_{\text{crit}}$ , and  $E$  denotes an ensemble expectation.

We thus obtain, for the crack which has grown over  $n (\gg 1)$  correlation lengths, the variance of local propagation velocity

$$E(V^2) \approx 2\eta^2 \hat{R}^2 \sum_{k=1}^n k^{-2p}. \quad (24)$$

The same type of result, proportional to the summation  $\sum_{k=1}^n k^{-2p}$ , is obtained for the variance of crack front slope,  $E(S^2)$ .

For the scalar theory,  $p = 1/2$ , and  $\sum_{k=1}^n k^{-2p}$  becomes  $\sum_{k=1}^n k^{-1}$ , which approaches a constant  $+\log(n)$ . Thus this reproduces, through a simplified development, the main feature of the Perrin and Rice (1994) results, namely, that  $E(V^2)$  [and also  $E(S^2)$ ] increases like a constant  $+\log(v_0 t/b)$  at large  $t$ .

For vectorial elasticity, with its persistent crack front waves,  $p = 0$  so that the summation  $\sum_{k=1}^n k^{-2p} = n$ . Thus,  $E(V^2)$  and  $E(S^2)$  grow with leading effect at large  $t$  that is directly proportional to  $v_0 t/b$ , i.e., to the number  $n$  of correlation lengths traversed, and hence to the distance of crack growth into the heterogeneous region. The vectorial elasticity case discussed here is that of a mode I crack constrained to lie in a plane. However, if for other modes, or for perturbations out of the plane, a persistent crack front wave could be shown to exist, then for similar reasons, the variances of  $V$  and  $S$  within the linear perturbation range should grow as  $v_0 t/b$ .

A full non-linear analysis is required to establish the ultimate limit to such fluctuations. Presumably, they do approach a finite amplitude, statistically stationary, distribution. It is not yet known if that finite amplitude will approach zero as the size of perturbation approaches zero or if it instead will always ultimately result in velocity fluctuations between zero and some high speed, perhaps  $v_{\text{limit}}$ . Simulation results for the scalar case with finite variations in  $G_{\text{crit}}$  by Rice *et al.* (1994), based on retaining the full non-linear form of  $g(v)$  in eqns (7) and (8), but on evaluating  $G_{\text{rest}}$  by the linearized perturbation expression, suggest that the perturbations of crack velocity can grow so large that the crack front can momentarily come to a complete halt at isolated positions along the front. Further, there was a tendency for such arrest zones to propagate laterally along the crack front, much like for the pulses shown in the small perturbation situation here.

These non-linear crack perturbation phenomena can, in principle, be studied by the spectral methodology used here. To do so in an illuminating way, which means with very long crack growth times before effects of the finite computational domain affect the results, will require its implementations on computer architectures with massive memory and highly parallel rapid processors.

It is known that smooth tensile fracture surfaces in glass (Wallner, 1939) and tungsten (Hull and Beardmore, 1966) can exhibit long-lived pulse markings, now called Wallner lines, produced by disturbances at the intersection of the main crack front and the specimen surface, or at internal heterogeneities. The crack front wave results shown in this paper, or perhaps some extension of them which explicitly includes small out-of-plane crack motion, may provide an explanation of Wallner lines.

## EXACT LINEARIZED ANALYSIS OF STATISTICS OF DISORDERED GROWTH

A more precise analysis of the statistics may be formulated following Perrin and Rice (1994), who derived the spatial correlation function and power spectral density

of  $A(z, t) \equiv a(z, t) - v_0 t$  in the scalar case. They describe a perturbation measure  $\tau(z, t)$  which is equivalent within linearization to

$$\tau(z, t) = \Delta G_{\text{crit}}(v_0 t, z) / [2G_{\text{crit},0}]. \tag{25}$$

Here  $\Delta G_{\text{crit}}(x, z)$  is a stationary random function with zero mean in the domain  $x > 0$ , and we assume  $\Delta G_{\text{crit}}(x, z) = 0$  in  $x < 0$  so that the crack enters the randomly heterogeneous zone with an initially straight front. The random distribution has correlation function

$$R_\tau(z_2 - z_1, x_2 - x_1) = E[\tau(z_1, x_1/v_0)\tau(z_2, x_2/v_0)] \tag{26}$$

for  $x_1, x_2 > 0$ .

Let the spacewise Fourier transform of  $\tau(z, t)$ , and of the linear perturbation response  $A(z, t)$  to it, be

$$[\tilde{\tau}(k, t), \tilde{A}(k, t)] = \int_{-\infty}^{+\infty} [\tau(z, t), A(z, t)] e^{-ikz} dz. \tag{27}$$

These must be related by an expression of the type

$$\tilde{A}(k, t) = - \int_{-\infty}^{+\infty} L(k\theta) \tilde{\tau}(k, t - \theta) d\theta, \tag{28}$$

where dimensional considerations show that the response kernel  $L$  can depend on  $k$  and  $t$  only in the product form  $kt$ .

The response  $L$  may be obtained from the full space and time Fourier transform  $\hat{A}(k, \omega)$  of  $A(z, t)$ , which satisfies an equation of the type  $\hat{A}(k, \omega) = \hat{H}(k, \omega) \hat{\tau}(k, \omega)$ , where the transfer function  $\hat{H}(k, \omega)$  is given for the scalar case by Perrin and Rice (1994). From it they showed that  $L(kt) = 2\alpha_0^2 c J_0(\alpha_0 k c t)$ . The  $\hat{H}(k, \omega)$  for the vectorial mode I case may be extracted from the Willis and Movchan (1995) perturbation solution in the way explained in eqns (21) and (22). However, the complexity of the expression for  $F(\omega/k, v_0)$  seems to preclude an explicit extraction of the response kernel  $L(kt)$  for that case although, because of the pole, we recognize the  $L(kt)$  should approach a non-zero periodically oscillating function, of frequency  $k\sqrt{c_r^2 - v_0^2}$ , at large  $kt$ .

We may now follow step by step the development of Perrin and Rice (1994), now phrased more generally in terms of the linear response functions  $L$  for either the scalar or vectorial case. Thus it follows by reproducing, in that more general context, the results of their Section 6 that the spatial power spectral density of the random process  $A(z, t)$  is

$$\begin{aligned} \psi_A(k, t) &\equiv \int_{-\infty}^{+\infty} E[A(0, t)A(z, t)] e^{-ikz} dz \\ &= \int_0^t \int_0^t L(k\theta_1) L(k\theta_2) \tilde{R}_\tau(k, v_0(\theta_2 - \theta_1)) d\theta_1 d\theta_2. \end{aligned} \tag{29}$$

Here  $\tilde{R}_\tau(k, x)$  is the Fourier transform of  $R_\tau(z, x)$ . As Perrin and Rice (1994) found,

even in the scalar case,  $\psi_A(k, t)$  diverges as  $t \rightarrow \infty$  due to the strong contribution along and near the diagonal  $\theta_1 = \theta_2$  of the region of integration. This feature is best seen by making the change of variables  $r = v_0(\theta_1 + \theta_2)/2$ ,  $s = v_0(\theta_2 - \theta_1)$ . Then

$$\psi_A(k, t) = \frac{1}{v_0^2} \int_0^{v_0 t} \left[ \int_{-2\min(r, v_0 t - r)}^{+2\min(r, v_0 t - r)} L\left(\frac{r-s/2}{v_0/k}\right) L\left(\frac{r+s/2}{v_0/k}\right) \tilde{R}_\tau(k, s) ds \right] dr. \quad (30)$$

The bracketed integral on  $s$  receives non-negligible (or in some cases non-zero) contributions only when  $|s|$  is of order of the correlation length  $b$  in the random fracture energy fluctuations, since  $\tilde{R}_\tau(k, s)$  is zero or insignificant at greater  $|s|$ . Hence the value of the double integral at large  $t$  is controlled by the variation of  $[L(kr/v_0)]^2$  with  $r$  at large  $r$ .

In the scalar case  $L(kr/v_0)$  inherits from its Bessel function dependence a behavior of type

$$L(kr/v_0) \propto \sqrt{v_0/\alpha_0} kr \cos(\alpha_0 kcr/v_0 + \text{constant}) \quad (31)$$

at large  $r$ , so that  $[L(kr/v_0)]^2$  integrates to a term which grows as  $\log(v_0 t)$  at large  $t$ . Hence the power spectral density  $\psi_A(k, t)$  for any  $k$  diverges as  $\log(v_0 t)$  in that case, as shown by Perrin and Rice (1994). For the vectorial case we understand on the basis of the persistent crack tip waves that

$$L(kr/v_0) \propto \cos(\sqrt{c_f^2 - v_0^2} kr/v_0 + \text{constant}) \quad (32)$$

at large  $r$ , so that the integral of  $[L(kr/v_0)]^2$  grows at large  $t$  in direct proportion to  $v_0 t$ . Hence we have the yet stronger divergence of  $\psi_A(k, t)$ , as  $t$  itself in that case. The spatial power spectral density of the crack front slope  $S(z, t) \equiv \partial a(z, t)/\partial z$  is  $\psi_S(k, t) = k^2 \psi_A(k, t)$ , so it is likewise divergent with  $t$ . These results are consistent with the simplified analysis of the last section.

## SUMMARY

We have used the spectral elastodynamic numerical methodology of Geubelle and Rice (1995) and a displacement–weakening cohesive fracture model to study the fluctuations of crack fronts induced by small heterogeneities in fracture energy. The cracks are constrained to propagate on a plane in a 3-D solid (Figs 1 and 4) and would grow with straight fronts in the absence of any perturbation.

Heterogeneity of critical fracture energy in the form of an isolated asperity is shown to create pulse-like disturbances of local crack propagation velocity, which propagate laterally along the moving crack front. For the model elastic theory, based on a scalar wave equation, the pulse amplitude is found to decay as  $t^{-1/2}$  well after the asperity encounter (Figs 5 and 6). That is in agreement with the results of linearized perturbation analysis of Rice *et al.* (1994) and Perrin and Rice (1994) for a singular crack growing with a constant fracture energy criterion in such a scalar solid.

For actual vectorial elasticity in the mode I tensile crack case, we find that the pulses do not decay, at least over the time scale of our simulation, and appear to represent a previously unrecognized type of persistent wave which propagates along

the crack front (Figs 7 and 8). Willis and Movchan (1995) gave a small perturbation solution for the singular mode I crack in vectorial elasticity. They did not develop details of the solution or discuss the crack motion according to any particular fracture criterion. However, Ramanathan and Fisher (1997) have developed details of the Willis–Movchan solution and shown that when it is applied to crack growth at constant fracture energy, there is indeed a persistent crack front wave implied, like that found in our simulation.

Even the (slowly) decaying pulse of the scalar model had been shown (Perrin and Rice, 1994) to imply continuously growing variances of crack front slope and local propagation velocity, in linearized perturbation analysis of growth into a region of small random fluctuation in critical fracture energy. In that case the variances were proven to grow with the logarithm of distance of propagation into the heterogeneous region. We present a statistical analysis here which confirms that result. It shows also that, because of the persistent crack front waves of actual vectorial elastodynamics, the growth of disorder is then yet more rapid. Variances of crack front slope and local propagation velocity, again within linearized perturbation theory, grow (to leading order) in direct proportion to distance of growth into the heterogeneous region. Crack front waves may also provide an explanation of persistent crack surface markings called Wallner lines.

### ACKNOWLEDGEMENTS

The studies were supported by the Office of Naval Research, Ship Structures Division, Solid Mechanics Program, through grant N00014-96-10777. Access to the CM-5 was made possible by NSF grant EAR 940004N of time at the National Center for Supercomputer Applications, Urbana, IL. We are grateful to Philippe Geubelle for discussion on the methodology and to Daniel Fisher and Sharad Ramanathan for discussions on the interpretation of results.

### REFERENCES

- Ben-Zion, Y. and Morrissey, J. W. (1995) A simple re-derivation of logarithmic disordering of a dynamic planar crack due to small random heterogeneities. *Journal of the Mechanics and Physics of Solids* **43**, 1363–1368.
- Cochard, A. and Rice, J. R. (1997) A spectral method for numerical elastodynamic fracture analysis without spatial replication of the rupture event. *Journal of the Mechanics and Physics of Solids*, in press.
- Eshelby, J. D. (1969) The elastic field of a crack extending non-uniformly under general anti-plane loading. *Journal of the Mechanics and Physics of Solids* **17**, 177.
- Freund, L. B. (1972) Crack propagation in an elastic solid subject to general loading, I, constant rate of extension, II, non-uniform rate of extension. *Journal of the Mechanics and Physics of Solids* **20**, 129–140, 141–152.
- Freund, L. B. (1990) *Dynamic Fracture Mechanics*. Cambridge University Press, Cambridge, U.K.
- Geubelle, P. H. and Rice, J. R. (1995) A spectral method for three-dimensional elastodynamic fracture problems. *Journal of the Mechanics and Physics of Solids* **43**, 1791–1824.
- Hull, D. and Beardmore, P. (1966) Velocity of propagation of cleavage cracks in tungsten. *Int. J. Fracture Mech.* **2**, 468–487.

- Kostrov, B. V. (1966) Unsteady propagation of longitudinal shear cracks. *Appl. Math. and Mech.* (English translation of *Prikl. Mat. i Mek.*) **30**, 1241–1248.
- Morrissey, J. W. and Geubelle, P. H. (1997) A numerical scheme for mode III dynamic fracture problems. *Int. J. Numer. Meth. Engng* **40**, 1181–1196.
- Morrissey, J. W. and Rice, J. R. (1996) 3D elastodynamics of cracking through heterogeneous solids: crack front waves and growth of fluctuations (Abstract). *EOS, Trans. Amer. Geophys. Union* **77**(46, Fall Meeting Suppl), F485.
- Movchan, A. B. and Willis, J. R. (1995) Dynamic weight functions for a moving crack. II. Shear loading. *Journal of the Mechanics and Physics of Solids* **43**, 1369–1383.
- Perrin, G. and Rice, J. R. (1994) Disorder of a dynamic planar crack front in a model elastic medium of randomly variable toughness. *Journal of the Mechanics and Physics of Solids* **42**, 1047–1064.
- Ramanathan, S. and Fisher, D. (1997) Dynamics and instabilities of planar tensile cracks in heterogeneous media. *Phys. Rev. Lett.* **79**, 877–880.
- Rice, J. R. (1980) The mechanics of earthquake rupture. *Physics of the Earth's Interior* (Proc. International School of Physics “Enrico Fermi”, Course 78, 1979; ed. A. M. Dziewonski and E. Boschi), Italian Physical Society and North-Holland Publ. Co., pp. 555–649.
- Rice, J. R., Ben-Zion, Y. and Kim, K.-S. (1994) Three-dimensional perturbation solution for a dynamic planar crack moving unsteadily in a model elastic solid. *Journal of the Mechanics and Physics of Solids* **42**, 813–843.
- Wallner, H. (1939) Linienstrukturen an bruchflächen. *Z. Physik* **114**, 368–378.
- Washabaugh, P. D. and Knauss, W. G. (1994) A reconciliation of dynamic crack velocity and Rayleigh wave speed in isotropic brittle solids. *Int. J. Fracture* **65**(2), 97–114.
- Willis, J. R. and Movchan, A. B. (1995) Dynamic weight functions for a moving crack. I. Mode I loading. *Journal of the Mechanics and Physics of Solids* **43**, 319–341.
- Willis, J. R. and Movchan, A. B. (1997) Three-dimensional dynamic perturbation of a propagating crack. *Journal of the Mechanics and Physics of Solids* **45**, 591–610.